

Carbon-grain sublimation: a new top-down component of protostellar chemistry

MEREL L.R. VAN 'T HOFF,¹ EDWIN A. BERGIN,¹ JES K. JØRGENSEN,² AND GEOFFREY A. BLAKE³

¹*Department of Astronomy, University of Michigan, 500 Church Street, Ann Arbor, MI 48109, USA*

²*Niels Bohr Institute, University of Copenhagen, Øster Voldgade 5-7, 1350 Copenhagen K., Denmark*

³*Division of Geological & Planetary Sciences, MC 150-21 California Institute of Technology Pasadena, CA 91125, USA*

ABSTRACT

Earth's carbon deficit has been an outstanding problem in our understanding of the formation of our Solar System. A possible solution would be the sublimation of carbon grains at the so-called soot line (~ 300 K) early in the planet-formation process. Here, we argue that the most likely signatures of this process are an excess of hydrocarbons and nitriles inside the soot line, and a higher excitation temperature for these molecules compared to oxygen-bearing complex organics that desorb around the water snowline (~ 100 K). Such characteristics have been reported in the literature, for example, in Orion KL, although not uniformly, potentially due to differences in observational settings and analysis methods of different studies or related to the episodic nature of protostellar accretion. If this process is active, this would mean that there is a heretofore unknown component to the carbon chemistry during the protostellar phase that is acting from the top down – starting from the destruction of larger species – instead of from the bottom up from atoms. In the presence of such a top-down component, the origin of organic molecules needs to be re-explored.

1. INTRODUCTION

One of the main goals in the fields of exoplanets and planet formation is to determine the composition of terrestrial, potentially habitable, planets and to link this to the composition of protoplanetary disks. A longstanding puzzle in this regard is the Earth's severe carbon deficit. Earth is four orders of magnitude depleted in carbon compared to interstellar grains, and two well-characterized comets 1P/Halley and 67P/Churyumov-Gerasimenko (hereafter, 67P) (e.g., Geiss 1987; Bergin et al. 2015; Rubin et al. 2019). The exact depletion is uncertain as a significant amount of carbon could be present in the Earth's core, but even generous upper limits suggest one to two orders of magnitude depletion for the bulk Earth (see e.g., Marty 2012; Fischer et al. 2020; Li et al. 2020, subm.). A similar amount of depletion is seen in CI chondrites that are thought to represent the most primitive material in the Solar System and otherwise reflect solar abundances in terms of composition (Wasson & Kallemeyn 1988). Moreover, this problem exists beyond the Solar System as carbon deficits in polluted white dwarfs are indicative of the

accretion of carbon-depleted rocky material (e.g., Jura 2006).

The only solution to this conundrum is that in the inner few au of planet-forming systems, carbon has to be in the gas phase instead of the refractory phase, and as such, becomes unavailable for accretion onto rocky bodies. Thus, there must be a mechanism to destroy carbon grains while leaving silicate grains intact. Furthermore, this must happen prior to planetesimal formation as it is much easier to destroy smaller grains than it is to break apart planetesimals and entirely ablate them. This points towards the early, embedded, phases in the evolution of young stars before significant grain growth sets in (i.e., the Class 0 and early Class I protostellar stages). As this mechanism is central to the supply of carbon to terrestrial worlds, constraining it is of fundamental importance. Carbon-grain destruction has been explored in the literature with a primary focus on oxidation (e.g., Finocchi et al. 1997; Lee et al. 2010; Gail & Tieloff 2017), but detailed models by Anderson et al. (2017) and Klarmann et al. (2018) suggest that this mechanism is ineffective.

Here, we focus on sublimation of refractory carbon grains at a location that can be labeled as the “soot line” (Kress et al. 2010). Although the specific molecular form of carbon in grains is unknown, the majority

of refractory carbon-rich solids are sublimating at temperatures between \sim 350 and 450 K (Nakano et al. 2003; Gail & Tieloff 2017; Li et al. 2020, subm.). If the process of carbon-grain sublimation is indeed active, this would mean that there is a heretofore unrecognized contributor to the rich carbon chemistry. This pathway acts from the top down, that is, starting from the destruction of larger molecules, instead of from the bottom up as in traditional gas and ice chemistry (see also Tielens 2011 for a discussion on top-down chemistry). In Sect. 2, we outline what the observational signatures of carbon-grain sublimation could be. In Sect. 3 we review whether there is current evidence that this process is happening and in Sect. 4 we discuss future steps to establish whether carbon-grain sublimation is a common process during star- and planet formation.

2. SIGNATURES OF CARBON-GRAIN SUBLIMATION AND TOP-DOWN CHEMISTRY

In hot cores, it is common to think of molecular abundance changes across the water snowline (\sim 100 K) as many complex molecules have binding energies similar to water. A simple approach would therefore be to look for an additional change in the chemical structure at the temperature of carbon-grain sublimation (see Fig. 1, top panel). The questions then become what these signatures are and where to look for them.

Before we explore these issues we need to address the sublimation temperature of carbonaceous grains, which is \sim 425 K for pressures representing the regions in the solar nebula disk at a few au from the Sun (i.e., the formation zone for meteoritic material) (Nakano et al. 2003; Gail & Tieloff 2017; Li et al. 2020, subm.). This number is based upon the recent analysis of Li et al. (2020, submitted) who note that meteoritic constraints bound the sublimation temperature of the main carbon carrier to be within 200 - 650 K. Drawing upon the laboratory experiments of cometary organic analogs of Nakano et al. (2003) we adopt their number of 425 K. Sublimation has a well characterized exponential relation between pressure and temperature (e.g., the Clapeyron-Classius equation). To obtain a rough estimate of the sublimation temperature at hot core pressures we use the dP_{vap}/dT (where P_{vap} is the vapor pressure) relations of PAHs characterized in the lab (Goldfarb & Suuberg 2008; Aslam Siddiqi et al. 2009) and assume that only the density of H₂ and temperature changes (i.e., abundance is constant). Based on these dependencies (see also, Bergin & Cleeves 2018), we obtain a (very) rough estimate of \sim 300 K for the temperature of carbon-grain destruction at reduced pressures (densities of 10^7 – 10^8 H₂ cm⁻³, 300 K; P \sim 10^{-13} bar) in the in-

ner region around protostars, compared to the inner disk (P(1 au) \sim 10^{-6} bar; D’Alessio et al. 2005). We note that strictly speaking the above relations refer to pure ices and the temperature of the medium. In this case the temperature refers to the gas and dust temperature which are coupled in these regions.

2.1. Excess carbon and nitrogen

The most obvious effect of carbon-grain sublimation is a flooding of the gas with carbon. Since most of the oxygen is expected to be locked up in water (Bergin & Snell 2002; Caselli et al. 2012), this carbon enters gas that is rich in hydrogen, nitrogen (mostly in N₂), CO, and H₂O. Carbon will therefore most likely react to form hydrocarbons and nitriles (molecules with a C≡N bond, such as HCN and CH₃CN) as shown in chemical models of protoplanetary disks in which the destruction of carbon grains is simulated by an excess of C⁺ (Wei et al. 2019). This gets complicated by the fact that some hydrocarbons and nitriles also form bottom up in the gas or ice.

However, based on the cometary inventory, there is significantly more nitrogen contained in refractories than in volatile ices (Rice et al. 2018; Rubin et al. 2019). Carbon is similar to nitrogen in comet 67P, and both are distinct from oxygen, which is twice as abundant in volatile ices as in refractory organics (Rubin et al. 2019). The refractory C/N elemental ratio in carbonaceous chondrites, comets 1P/Halley and 67P is \sim 5-30 (Bergin et al. 2015; Jessberger et al. 1988; Rubin et al. 2019). Assuming 50% of the elemental carbon is in refractory form (150 ppm with respect to H; Mishra & Li 2015) then the destruction of carbon grains releases 5-30 ppm of refractory nitrogen into the gas. This is about 10-50% of the present day cosmic nitrogen abundance (Nieva & Przybyilla 2012).

Recently, evidence of the presence of ammonium salts was reported in comet 67P, providing an additional nitrogen-bearing component (Altwegg et al. 2020; Poch et al. 2020). These works derive an upper limit of 40 wt% for the mass fraction of ammonium salts, but depending on the composition of the salts, a 10 wt% mass fraction can be enough for a solar C/N ratio (\sim 3.4, Lodders 2010) for the entire comet. In these cases, \sim 10% to almost 40% of all nitrogen, respectively, would be in refractories. Sublimation of carbon grains with these compositions would then release 9-36 ppm of refractory nitrogen. Furthermore, the desorption temperature of ammonium salts (roughly 200-250 K, Clementi & Gayles 1967; Raunier et al. 2004; Bossa et al. 2008; Danger et al. 2011; Vinogradoff et al. 2011; Noble et al. 2013; Bergner et al. 2016) is higher than that of water and comparable

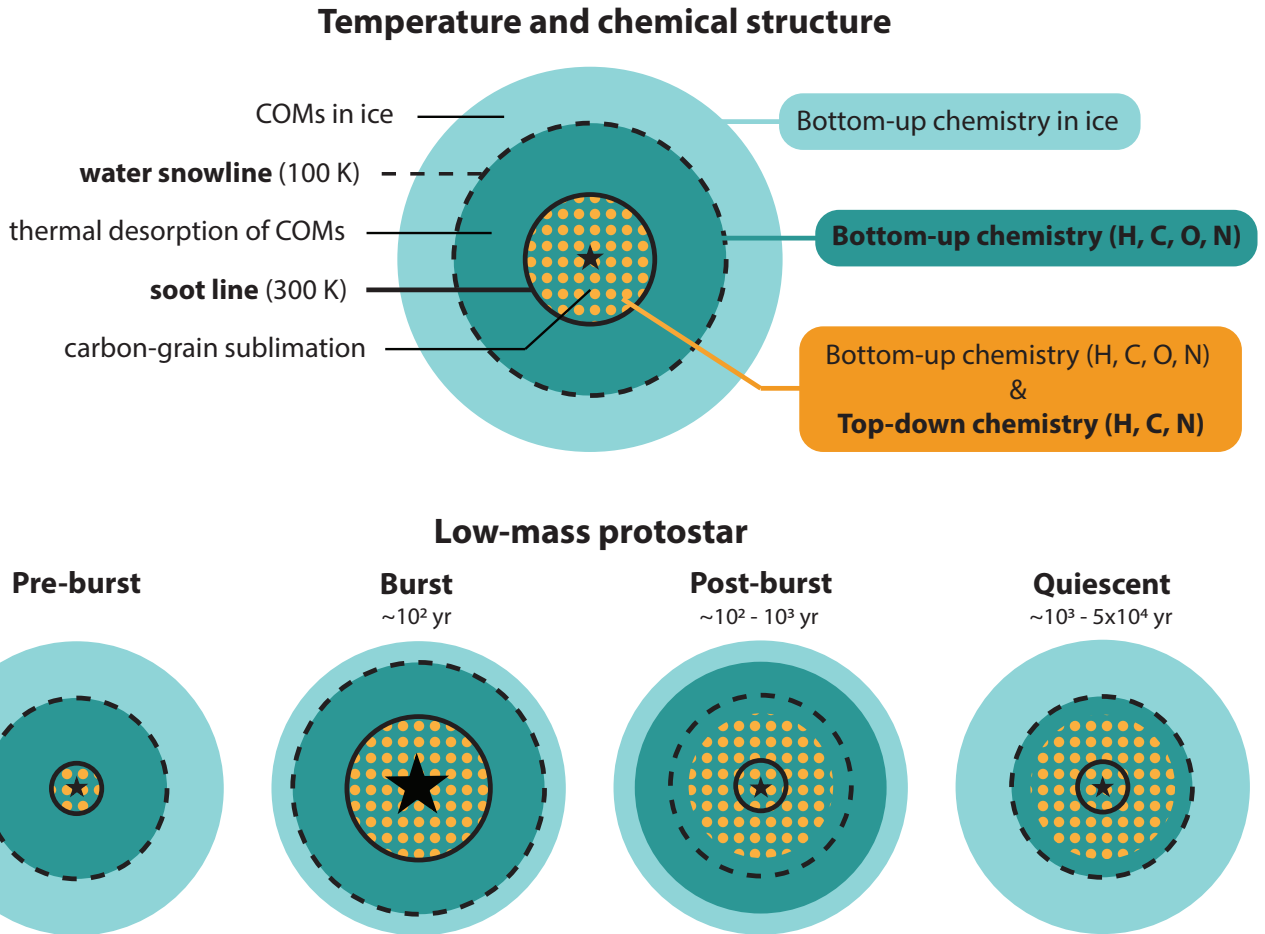


Figure 1. *Top panel:* Schematic of the temperature and chemical structure around a protostar (not to scale). In the outer most part of the envelope, complex organic molecules (COMs) are present in the ice, where they have been formed, for example, through a sequence of hydrogenation reactions starting with the hydrogenation of CO (that is, bottom up). When the temperature exceeds ~ 100 K at the water snowline (dashed black line; a few 10s of au for $1 L_\odot$), the COMs desorb off the dust grains and may continue to react in the gas phase. Inside the soot line (~ 300 K at a few au for $1 L_\odot$; solid black line), carbon grains sublime, providing a top-down component to the chemistry (depicted with orange dots) that enriches the gas with carbon and nitrogen. *Bottom panels:* Schematic of the evolution of the temperature and chemistry for a low-mass protostar that undergoes an accretion burst, using the same lines and color coding as in the *top panel*. Depending on the strength of the burst, the soot line may or may not shift past the quiescent snowline location. In the scenario illustrated here, the soot line does not shift past the quiescent snowline. The duration of the different phases is indicated above the panels. See Sect. 2.3 for details.

to that of refractory carbon. In the outlined scenarios, $\sim 60\text{--}90\%$ of all nitrogen is expected to be in ammonium salts, so these salts could deliver an additional amount of nitrogen to the gas inside the soot line.

Sublimation of carbon grains would thus lead to an excess of carbon and nitrogen in the gas phase (see Fig. 1, top panel). The exact form in which these elements will be released (e.g., N along with C or NH with CH or C with CN or larger fragments) is unknown. If polycyclic aromatic hydrocarbons (PAHs) are freed, this carbon will not be readily available for gas-phase chemistry. However, both low and high-mass protostars lack PAH emission (van Dishoeck & van der Tak 2000; Geers et al.

2009), while according to radiative transfer models, PAH emission should always be detectable in Herbig Ae/Be disk/envelope systems if they are present (Manske & Henning 1999). It seems therefore unlikely that the 90% of carbon that is missing in inner Solar System bodies is present in PAHs. Another unknown is which molecules will be formed exactly and in what amounts. However, cometary compositions indicate that the top-down signal could dominate over the bottom-up contribution. Finally, it is possible that a highly refractory component might exist (e.g. SiC), but the carbon deficit in even the most primitive meteorites requires significant carbon grain destruction to the order of 90% (Bergin et al.

2015) at the time these materials are isolated from the gaseous nebula.

2.2. Isotopic fractionation

In the ISM, only $< 17 \pm 11\%$ of all nitrogen is contained in refractories, while this is 20 – 85% in comets (Jensen et al. 2007; Bergin et al. 2015; Rice et al. 2018; Rubin et al. 2019). At some point during the star-formation process, nitrogen must thus be captured and placed into refractory material. The detection of benzonitrile in dark clouds suggest that there may be a pathway to do this at low temperatures (McGuire et al. 2018). Signatures of low-temperature formation, such as isotope fractionation, may therefore be present in the nitrogen that comes free upon grain sublimation. This may distinguish molecules formed through this top-down process from species formed in the gas through a bottom-up pathway. However, complex nitrogen-bearing molecules formed in the ice may carry similar fractionation features.

2.3. Higher excitation temperature for N-COMs

Observing the predicted excess of hydrocarbons and nitriles inside the soot line would require spatially resolving the $\gtrsim 300$ K region. Protostars are the best sources to target because 1) the sublimation has to happen early in the planet-formation process and 2) the soot line is at larger distances than in protoplanetary disks due to the higher accretion rates of these younger systems and their different density structures that result in less shielding of the stellar irradiation. If the soot line is not resolved, a comparison of the excitation temperatures of nitrogen-bearing and oxygen-bearing complex organic molecules (N-COMs and O-COMs, respectively) could still indicate whether carbon-grain sublimation is taking place: the excitation temperatures of N-COMs, enhanced at temperatures $\gtrsim 300$ K, will be higher than those of O-COMs that will be uniformly present inside the water snowline ($\gtrsim 100$ K; Fig. 1, top panel). In case of a large abundance of N-COMs formed through bottom-up chemistry outside the snowline, N-COM emission may be characterized by a hot ($\gtrsim 300$ K) and cold component. However, whether a temperature signal can be observed will depend on the extent of the $\gtrsim 300$ K region within the telescope beam, and is thus not as good a diagnostic as spatial differentiation.

A separate complication is that the temperature profile itself will change as the young star evolves. Accretion is episodic (see e.g., Hartmann & Kenyon 1996; Evans et al. 2009; Scholz et al. 2013) and enhanced accretion rates cause the luminosity and thus the temperature to increase. This leads to chemical changes due to

the soot line and snowlines moving outward (e.g., Lee 2007; Visser & Bergin 2012 and see Fig 1, burst panel). Catching a protostar during such a burst phase would thus make the detection of grain-sublimation signatures easier. Post-burst, the dust and gas temperature rapidly decay (~ 1 year) to levels associated with the quiescent protostellar luminosity (Johnstone et al. 2013). However, chemical changes persist and sublimated molecules remain in the gas phase in the inner envelope for a depletion timescale of $\sim 10^2$ – 10^3 years (Lee 2007; Visser & Bergin 2012). Thus it is possible that a chemical signature of carbon-grain sublimation is present even in cases where the temperature signature is absent (see Fig. 1, post-burst panel).

If the soot line does not get shifted past the quiescent snowline location, the species formed inside the extended soot line will remain present in the gas phase (see Fig. 1, quiescent panel). Alternatively, if the burst pushes the soot line beyond the quiescent snowline location, newly formed species outside the quiescent snowline will also freeze out. In this scenario there will be no spatial differentiation between gas-phase N-COMs and O-COMs as they both extend out to the quiescent snowline location. During the quiescent phase, it will thus depend on the burst location of the soot line compared to the quiescent location of the snowline whether there is a spatial difference between N-COMs and O-COMs. If the spatial difference is small or absent, the only signal of carbon-grain sublimation may be an enhanced abundance of N-COMs. Whether a clear signature can be observed for an individual protostar will thus depend on the time since its last accretion burst and the strength of that, and potentially previous, bursts.

3. OBSERVATIONAL EVIDENCE FOR CARBON-GRAIN SUBLIMATION AND TOP-DOWN CHEMISTRY

An increased abundance of hydrocarbons and nitriles inside the soot line, a smaller spatial extent for these species compared to oxygen-bearing COMs and/or higher excitation temperatures than O-COMs are thus expected signatures for sublimation of carbon grains. A clear manifestation of these signatures may be complicated by the occurrence of accretion bursts and the presence of N-COMs formed through bottom-up chemistry. Is there any evidence in the literature that this process is indeed taking place?

3.1. N-COM/O-COM spatial distribution and abundance correlation

Probably the most well-known example of N-COMs tracing different regions than O-COMs is Orion KL,

where the N-COMs are associated with the hot core while O-COMs are predominantly found toward the compact ridge (e.g., [Blake et al. 1987](#); [Friedel & Snyder 2008](#)). The total abundance of N-COMs in the hot core is more than an order of magnitude higher than in the colder compact ridge ([Crockett et al. 2014](#)). If what we are seeing here is the results of carbon grain sublimation, this process may thus indeed result in observable enhancements of N-COMs.

A similar spatial differentiation was also observed toward the high-mass star-forming region W3, where N-COMs are found only toward the W3(H₂O) core while O-COMs are present in both the W3(H₂O) and W3(OH) regions ([Wyrowski et al. 1999](#)), and G34.26+0.15, where emission from N- and O-COMs peak at different positions within the core ([Mookerjea et al. 2007](#)). Recent high-resolution observations ($\leq 0.5''$) reveal differences in AFGL 2591 VLA 3 ([Jiménez-Serra et al. 2012](#); [Gieser et al. 2019](#)), AFGL 4176 ([Bøgelund et al. 2019](#)), G35.20 core B ([Allen et al. 2017](#)), and G328.2551-0.5321 ([Csengeri et al. 2019](#)). In these high-mass sources, the N-COMs are found to peak on source, while the O-COMs peak offset from the central protostar. In addition, [Fayolle et al. \(2015\)](#) find that the N-COMs are generally concentrated toward the source centers in the three massive young stellar objects NGC 7538 IRS9, W3 IRS5 and AFGL490, while O-COM emission is more extended.

A hint of more compact emission from N-COMs than O-COMs is also observed for the disk around the outbursting star V883-Ori ([Lee et al. 2019](#)). This result is tentative, because due to the vertical temperature structure of disks and the dust being optically thick in the inner ~ 40 au in this system ([Cieza et al. 2016](#)) we may be seeing effects in the disk surface layers rather than the inner-disk midplane.

However, the spatial differentiation between N-COMs and O-COMs is not always black and white. For example, the O-COMs ethylene glycol ((CH₂OH)₂) and acetic acid (CH₃COOH) have a spatial distribution in Orion KL different from most other O-bearing molecules ([Brouillet et al. 2015](#); [Favre et al. 2017](#)) and the overall distribution of acetone ((CH₃)₂CO) is similar to that of ethyl cyanide (C₂H₅CN) ([Peng et al. 2013](#)).

Another hint of a difference between N-COMs and O-COMs is found when comparing molecular abundances. Abundances of O-COMs are often found to be correlated, while N-COMs either tend to show stronger correlations with other N-COMs rather than O-COMs, or show no correlation with any other molecule (e.g., [Bisschop et al. 2007](#); [Bergner et al. 2017](#); [Suzuki et al. 2018](#)). This is also not uniform as, for example, C₂H₃CN and C₂H₅CN were found to be correlated with CH₃OCH₃ by

[Fontani et al. \(2007\)](#), and [Belloche et al. \(2020\)](#) found a strong correlation between CH₃OH and CH₃CN. However, these results should be regarded with caution, as a correlation across sources does not necessarily reflect an actual chemical relationship but may also reflect underlying physical differences (e.g., temperatures, column densities or simply variations in the reference species).

3.2. Excitation temperature of N-COMs and O-COMs

Differences in excitation temperatures of N-COMs compared to O-COMs have been observed for Orion KL, with the N-COMs tracing hotter gas (~ 300 K) than the O-COMs ([Crockett et al. 2015](#)). The latter are consistent with sublimation alongside water around ~ 100 K. A similar picture emerges for Sgr B2(N₂), although the temperature differences are smaller ([Belloche et al. 2016](#)). On the other hand, O-COMs toward IRAS 16293–2422 B can be divided in two groups based on their excitation temperature (~ 125 K versus ~ 300 K; [Jørgensen et al. 2018](#)), consistent with different binding energies. N-COMs generally have excitation temperatures of 100–150 K ([Calcutt et al. 2018a,b](#)), but a high-temperature component may be hidden inside the unresolved soot line or by the optically thick dust.

To assess whether a difference in excitation temperature is a widespread phenomenon, we compiled an overview of the existing literature that reports excitation temperatures for at least one N-COM and one O-COM. Because not all studies observe the same molecules, Fig. 2 (top panel, and see also Table 1) shows the highest reported excitation temperature for N-COMs versus that of O-COMs for each source in a particular study. Molecules with less than 5 atoms and molecules containing both nitrogen and oxygen, like HNCO and NH₂CHO, are excluded. While there clearly are a large number of cases where a higher excitation temperature is reported for N-COMs than for O-COMs (64 out of 144 entries; 44%), this is certainly not always the case. Possible explanations will be discussed in Sect. 4.

4. DISCUSSION AND OUTLOOK

The spatial differentiation between N-COMs and O-COMs has been a longstanding problem ([Blake et al. 1987](#)). Initially, this was attributed to different ice compositions, because the relative amount of ammonia (NH₃) ice had a large impact on the CH₃CN/CH₃OH ratio in the chemical models from [Charnley et al. \(1992\)](#) and [Rodgers & Charnley \(2001\)](#). However, more recent models do not predict a correlation between the CH₃CN/CH₃OH gas ratio and the NH₃/CH₃OH ice ratio ([Garrod 2013](#)), consistent with observations of both low- and high-mass protostars ([Fayolle et al. 2015](#);

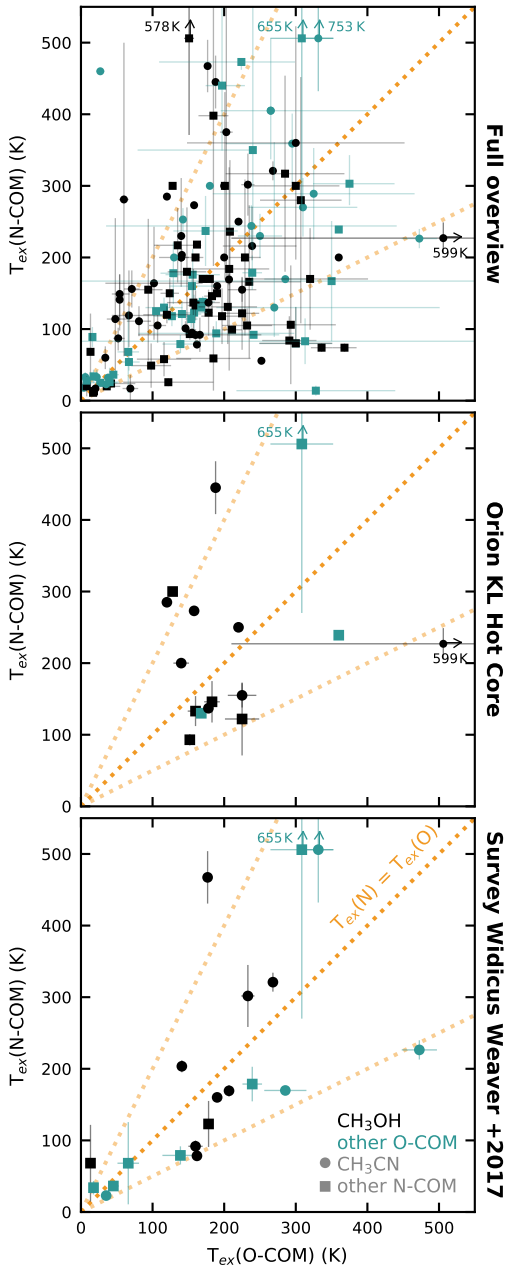


Figure 2. Highest excitation temperature among all nitrogen-bearing COMs versus that among all oxygen-bearing COMs reported in a study for a protostellar source. The *top panel* provides an overview of the literature, while the *middle panel* only shows results for Orion KL and the *bottom panel* only shows results from the survey by [Widicus Weaver et al. \(2017\)](#). References are listed in Table 1. The shape of the symbols indicate whether the highest excitation temperature for the N-COMs is for CH_3CN (circle) or for another species (square). The color of the symbols indicate whether the highest excitation temperature for the O-COMs is for CH_3OH (black) or for another species (teal). The dashed lines mark where the excitation temperature for N-COMs is twice that, equal to, and half of the O-COMs.

[Bergner et al. 2017](#)). Another explanation given in the literature is based on a difference in temperature between regions in combination with a different warm-up timescale, hence evolutionary stage (e.g., [Caselli et al. 1993](#); [Garrod et al. 2008](#); [Allen et al. 2018](#)).

Here, we suggest the thermal destruction of carbon grains inside the soot line (~ 300 K) as the underlying reason for the differences in distribution between N-COMs and O-COMs: regions rich in N-COMs are currently heated to temperatures above ~ 300 K, or have been in the past. While a different thermal history and evolutionary stage may explain the spatial differentiation and differences in excitation temperature, only carbon-grain sublimation can simultaneously explain the low carbon and nitrogen content of the Earth and CI chondrites, and the carbon-depleted pollution seen in white dwarf atmospheres.

As outlined in Sect. 3 and visualized in Fig. 2, a coherent picture indicating that carbon-grain sublimation is a common phenomenon during star formation does not yet exist. A complicating factor that could contribute to the non-uniformity in observed spatial distributions and abundance correlations, is that carbonaceous material could contain a small amount of oxygen. For example, about 25% of elemental oxygen is unaccounted for in the interstellar medium (e.g., [Whittet 2010](#); [Poteet et al. 2015](#)). There is some insight here from meteorites, as insoluble organic matter contains 22 O atoms for every 100 C atoms ([Remusat 2014](#)), which is roughly consistent with interstellar inferences. Thus, there is likely some oxygen-bearing organic material released as carbon grains are ablated.

Figure 2 displays a wide spread in excitation temperatures derived for both N-COMs and O-COMs (from a few K up to > 500 K). In addition, there is no clear correlation between the highest temperature for N-COMs and that for O-COMs, as N-COMs can be more than twice as hot as O-COMs but also more than twice as cold. The spread in excitation temperatures could be due to the heterogeneity of observations and analysis methods (see Fig. 2, middle panel, for an overview of studies toward Orion KL). Besides different spatial resolutions with respect to the size of the soot line, a relevant difference between studies is the covered wavelength range, as this determines which molecules are observed, the number of lines per molecule and the upper level energies of these lines. The latter can complicate conclusions about the spatial extent of a molecule, as even typical hot-core molecules, such as CH_3OH and CH_3CN , can be observed in the outer envelope when observing low-energy transitions (e.g., [Öberg et al. 2013](#)). In addition, these molecules often require both a hot and cold com-

ponent to explain observations, and this hot component could be missed when only lines with low upper level energies are targeted.

Furthermore, differences could result from different analysis techniques. In general, excitation temperatures are derived from rotational diagrams or from fitting the observed spectrum, but different assumptions about beam dilution and/or optical depth could give significantly different results (see e.g., Gibb et al. 2000). Finally, rotational temperatures can be higher than the kinetic temperature due to optical depth effects and/or infrared pumping (see e.g. Churchwell et al. 1986) and for large-scale single-dish studies the critical density and dipole moment of a species may be more important for the excitation than the temperature. Equal or lower excitation temperatures for N-COMs therefore do not necessarily indicate that carbon-grain sublimation is not occurring.

However, also systematic surveys do not present a uniform picture (see Fig. 2, bottom panel, for results from the survey by Widicus Weaver et al. 2017). The spread could illustrate that the soot line is not resolved in all sources, but sources with higher N-COM excitation temperatures span the entire luminosity and distance range among the high-mass sources in the sample. Another explanation could therefore be that a clear signature of carbon-grain sublimation may not be present for all sources. The episodic nature of the protostellar accretion could erase the spatial difference between N-COMs and O-COMs as well as differences in their excitation temperature (see Fig. 1). The fraction of sources in the post-burst phase (with the O-COMs spatially more extended than the N-COMs) is equal to the freeze-out timescale divided by the burst interval. The O-COMs have desorption temperatures similar to water, so their freeze-out timescale is \sim 1000 years (Visser et al. 2015). Several studies estimate that the burst interval is 20,000–50,000 years (e.g., Scholz et al. 2013; Jørgensen et al. 2015), while Hsieh et al. (2019) derive an interval of \sim 2400 years during the Class 0 phase. This means that we would expect 2–5% up to 40% of protostars in the post-burst phase. These numbers are not inconsistent with the number of studies finding higher excitation temperatures for N-COMs than for O-COMs in Fig. 2. A caveat here is, however, that it is unclear whether burst statistics for low-mass sources also ap-

ply for high-mass sources, which make up the majority (80%) of Fig. 2.

To unambiguously establish the presence of carbon-grain sublimation, large systematic surveys are thus required that spatially probe the soot line as well as cover a large number of lines with a range of upper level energies of many different molecular species. Chemical models incorporating the thermal destruction of carbon grains (such as done for protoplanetary disks by Wei et al. 2019) could help indicate what species are good indicators. The best candidates to establish the occurrence of carbon grain sublimation are sources with a clear spatial differentiation between N- and O-COMs (as listed in Sect. 3.1). A deep spectral survey and detailed analysis (e.g., of warm hydrocarbons) could reveal whether the observed distributions are consistent with suggested accretion shocks at the disk-envelope interface or with sublimation of carbon grains. Although the study of low-mass sources may be more appropriate to understand the formation of the Solar System and its analogs, the larger >300 K region makes high-mass sources the more accessible astrochemical laboratories.

If carbon grain sublimation is happening, it would mean that there is an unexplored top-down component to protostellar chemistry, that starts from the destruction of larger structures instead of from atoms. The implications for astrochemistry, the origin of organic molecules and carbon delivery to terrestrial worlds then needs to be re-explored.

ACKNOWLEDGMENTS

We would like to thank the referee and Ewine van Dishoeck for positive feedback that has improved this paper. M.L.R.H. acknowledges support from the Michigan Society of Fellows. E.A.B. acknowledges funding from NSF grant AST 1907653 and NASA grant XRP 80NSSC20K0259. J.K.J. acknowledges support by the European Research Council (ERC) under the European Union’s Horizon 2020 research and innovation programme through ERC Consolidator Grant “S4F” (grant agreement No 646908). G.A.B. acknowledges support from the NASA XRP (NNX16AB48G) and Astrobiology (NNX15AT33A) programs.

Table 1. Overview of literature presenting excitation temperatures for both N- and O-COMs in protostars.

Source name	Source type	$T_{\text{ex}}(\text{N-COM})^a$ (K)	$T_{\text{ex}}(\text{O-COM})^b$ (K)	$T_{\text{ex}}(\text{O-COM})^c$ (K)	$T_{\text{ex}}(\text{CH}_3\text{OH})^d$ (K)	Sign of CGS ϵ	Telescope	Analysis method f	Reference
AFGL 2591 VLA 3	High mass	150 \pm 20	124 \pm 12	n/a	...	yes	SMA	RD	Jiménez-Serra et al. (2012)
...	...	218 \pm 2	162 \pm 2	199 \pm 1	...	yes	IRAM 30m + NOEMA ALMA	M	Gieser et al. (2019)
AFGL 4176	High mass	270 \pm 40	310 \pm 75	...	120 \pm 15	...	IRAM 30m + SMA	M	Bøgholm et al. (2019)
AFGL 490	High mass	164 \pm 78	102 \pm 67	yes	IRAM 30m + SMA	RD	Fayolle et al. (2015)
B1-a	Low mass	33 \pm 9	22 \pm 5	...	n/a	yes	IRAM 30m	RD	Bergner et al. (2017)
B1-c	Low mass	18 \pm 2	4 \pm 1	...	n/a	yes	IRAM 30m	RD	Bergner et al. (2017)
B5 IRS 1	Low mass	11 \pm 2	17 \pm 2	n/a	IRAM 30m	RD	Öberg et al. (2014); Bergner et al. (2017)
Cep E-A	Int. mass	32 \pm 4	37 \pm 1	IRAM 30m + NOEMA	RD	Ospina-Zamudio et al. (2018)
DR21(OH)	High mass	55	252	...	27 \pm 5	...	OSO	RD	Kalenskii & Johansson (2010a)
...	...	79 \pm 11	138 \pm 24 ₁₄	56 \pm 2	92 \pm 2	...	CSO	M	Widicus Weaver et al. (2017)
G9.62+0.19	High mass	119 ₄₃ ⁶²	67 ₂₃ ⁵⁷	yes	JCMT	M	Hatchell et al. (1998)
G10.47+0.03	High mass	87 ₁₆ ¹⁴	52 ₆ ⁶	yes	JCMT	M	Hatchell et al. (1998)
...	...	176 \pm 35	156 \pm 37	n/a	n/a	yes	IRAM 30m	RD	Fontanini et al. (2007)
...	...	753 \pm 72	331 \pm 20	...	258 \pm 1	yes	CSO	M	Widicus Weaver et al. (2017)
G10.62-0.38	High mass	398 \pm 209	185 \pm 20	n/a	...	yes	Nobeyama	RD	Suzuki et al. (2018)
...	...	398 \pm 209	185 \pm 20	n/a	...	yes	Nobeyama	RD	Suzuki et al. (2018)
...	...	217 \pm 51	135 \pm 32	n/a	Nobeyama	RD	Suzuki et al. (2019)
...	...	166 \pm 106	235 \pm 71	n/a	ALMA	RD	Suzuki et al. (2019)
G12.21-0.10	High mass	89 \pm 13	16 \pm 1	n/a	n/a	yes	IRAM 30m	RD	Fontanini et al. (2007)
G12.89+0.49	High mass	78 \pm 4	161 \pm 3	165 \pm 23	n/a	yes	SMA	M	Wong & An (2018)
G12.91-0.26	High mass	24	42 ₁₅ ³³	n/a	CSO	M	Widicus Weaver et al. (2017)
G16.86-2.16	High mass	122 \pm 31	178 \pm 4	116 \pm 5	Nobeyama 45m + ASTE	RD	Taniguchi et al. (2018)
G19.61-0.23	High mass	20	36 ₉ ¹⁸	n/a	CSO	M	Widicus Weaver et al. (2017)
...	...	123 \pm 24	158 \pm 17	n/a	n/a	...	IRAM 30m	RD	Fontanini et al. (2007)
...	...	578 \pm 134	151 \pm 6	n/a	...	yes	SMA	RD	Qin et al. (2010)
...	...	467 \pm 35	176 \pm 2	yes	CSO	M	Widicus Weaver et al. (2017)
G24.33+00.11 MM1	High mass	301 \pm 42	233 \pm 8	yes	CSO	M	Widicus Weaver et al. (2017)
G24.78+0.08	High mass	99 ₀ ⁵	211 \pm 13	n/a	JCMT + IRAM 30m	RD	Bisschop et al. (2007)
...	...	203 \pm 7	140 \pm 1	yes	CSO	M	Widicus Weaver et al. (2017)
G28.28-0.36	High mass	13	18 ₃ ⁵	n/a	Nobeyama 45m + ASTE	RD	Taniguchi et al. (2018)
G29.96-0.02	High mass	114 ₈₀ ⁴⁰	48 ₁₁ ¹⁷	yes	JCMT	M	Hatchell et al. (1998)
...	...	121 \pm 17	141 \pm 26	n/a	n/a	...	IRAM 30m	RD	Fontanini et al. (2007)
G31.41+0.31	High mass	149 ₃₆ ²⁷	54 ₁₀ ¹³	yes	JCMT	M	Hatchell et al. (1998)
...	...	118 \pm 13	127 \pm 25	n/a	n/a	...	IRAM 30m	RD	Fontanini et al. (2007)
...	...	105 ₀ ²³	232 \pm 34	n/a	JCMT	RD	Isokoski et al. (2013)
...	...	80 ₀ ⁵⁰	300 \pm 50	n/a	200 \pm 50	...	JCMT	M	Isokoski et al. (2013)
...	...	320 \pm 12	268 \pm 4	yes	CSO	M	Widicus Weaver et al. (2017)

Table 1 *continued*

Table 1 (*continued*)

Source name	Source type	$T_{\text{ex}}(\text{N-COM})$	a (K)	$T_{\text{ex}}(\text{O-COM})$	b (K)	$T_{\text{ex}}(\text{CH}_3\text{CN})$	c (K)	$T_{\text{ex}}(\text{CH}_3\text{OH})$	d (K)	Sign of CGS e	Telescope	Analysis method f	Reference
...	...	59 ± 44	185 ± 51	n/a	Nobeyama	RD	Suzuki et al. (2018)
...	...	184 ± 141	207 ± 55	n/a	ALMA	RD	Suzuki et al. (2019)
G34.26+0.15	High mass	74 ± 5	368 ± 16	n/a	JCMT	RD	MacDonald et al. (1996)
...	...	74 ± 5	336 ± 14	n/a	JCMT	RD	MacDonald et al. (1996)
...	...	141 ₄₂ ³⁴	54 ₂ ³	yes	JCMT	M	Hatchell et al. (1998)
...	...	130 ± 13	116 ± 25	n/a	n/a	...	yes	IRAM 30m	RD	Fontani et al. (2007)
...	...	300 ± 130	201 ± 4	298 ± 8	yes	SMA	RD	Fu & Lin (2016)
...	...	160 ± 3	190 ± 1	CSO	M	Widicus Weaver et al. (2017)
...	...	167 ± 83	350 ± 412	n/a	196 ± 42	Nobeyama	RD	Suzuki et al. (2018)
...	...	49 ± 30	98 ± 27	n/a	Nobeyama	RD	Suzuki et al. (2018)
G35.03+0.35 A	High mass	216 ₁₆ ⁵⁴	239 ₄₀ ⁶¹	ALMA	M	Allen et al. (2017)
G35.20-0.74 N A	High mass	359 ₅₄ ⁴¹	295 ₅₂ ⁵²	227 ₇₃ ⁷³	yes	ALMA	M	Allen et al. (2017)
G35.20-0.74 N B3	High mass	47 ₃₀ ⁷⁴	224 ₁₄ ⁷⁴	213 ₄₇ ²⁷	189 ± 14	yes	ALMA	M	Allen et al. (2017)
G45.47+0.05	High mass	68 ± 52	13 ± 0	n/a	yes	CSO	M	Widicus Weaver et al. (2017)
G75.78+0.34	High mass	91 ± 7	159 ± 9	CSO	M	Widicus Weaver et al. (2017)
G327.3-0.60	High mass	303 ₂₉ ³⁹	375 ₅₀ ⁶²	282 ₆₅ ¹²⁵	180 ₁₁ ¹⁴	Herschel HIFI	RD	Gibb et al. (2000)
...	...	138 ₉ ⁷	170 ₁₈ ¹⁶	n/a	102 ± 10	Herschel HIFI	RD	Gibb et al. (2000)
...	...	135 ± 5	162 ₉ ¹¹	n/a	118 ₈ ⁶	Herschel HIFI	RD	Gibb et al. (2000)
G331.512-0.103	High mass	156 ± 25	71 ± 10	yes	APEX	RD	Mendoza et al. (2018)
IRAS 03255+3004	Low mass	13 ± 2	18 ± 4	n/a	IRAM 30m	RD	Öberg et al. (2014); Bergner et al. (2017)
IRAS 16233-2422	Low mass	54 ± 11	67 ± 14	n/a	n/a	IRAM 30m	RD	Cazaux et al. (2003)
IRAS 16233-2422 A	Low mass	160 ± 20	155 ± 31	120 ± 10	130 ± 26	yes	ALMA	M	Calcutt et al. (2018); Manigand et al. (2020)
IRAS 16233-2422 B	Low mass	300	300 ± 60	n/a	ALMA	M	Coutens et al. (2018); Jørgensen et al. (2018)
IRAS 18089-1732	High mass	84 ₃₃ ³³	291 ± 37	n/a	JCMT	RD	Isokoski et al. (2013)
...	...	80 ₀ ⁵⁰	300 ± 50	n/a	JCMT	M	Isokoski et al. (2013)
IRAS 20126+4104	High mass	230 ± 30	250 ± 30	...	n/a	PdBI	M	Palau et al. (2017)
IRAS 23238+7401	Low mass	33 ± 6	6 ± 2	...	n/a	yes	IRAM 30m	RD	Bergner et al. (2017)
IRDC-C9 Main	High mass	460	27 ± 5	...	n/a	yes	ALMA	RD	Beaklini et al. (2020)
L1448-C	Low mass	105 ± 23	107 ± 11	NOEMA	RD	Belloche et al. (2020)
L1489 IRS	Low mass	20 ± 13	8 ± 4	n/a	yes	IRAM 30m	RD	Öberg et al. (2014); Bergner et al. (2017)
L1527	Low mass	25 ± 4	27 ± 23	21 ± 2	13 ± 8	NRO 45m	RD	Yoshida et al. (2019)
L483	Low mass	28 ± 3	7 ± 13	n/a	n/a	yes	IRAM 30m	M	Agúndez et al. (2019)
NGC1333-IRAS2 A	Low mass	289 ± 63	325 ± 140	...	179 ± 62	PdBI	RD	Taquet et al. (2015)
...	...	130 ₄₀ ³⁰	270 ₈₀ ³⁰	...	140 ± 20	PdBI	RD	Taquet et al. (2015)
NGC1333-IRAS2 A1	Low mass	200 ± 108	229 ± 21	161 ± 17	NOEMA	RD	Belloche et al. (2020)
NGC1333-IRAS4 A	Low mass	360 ± 162	300 ± 151	yes	PdBI	RD	Taquet et al. (2015)
...	...	200 ₄₀ ¹¹⁰	140 ± 30	yes	PdBI	RD	Taquet et al. (2015)
NGC1333-IRAS4 A2	Low mass	280 ± 171	307 ± 56	142 ± 13	305 ± 52	NOEMA	RD	Belloche et al. (2020)
NGC1333-IRAS4 B	Low mass	14 ± 6	328 ± 110	n/a	NOEMA	RD	Belloche et al. (2020)
NGC 2264 CMM3	High mass	25 ± 4	122 ± 62	9 ± 4	Nobeyama 45m / ASTE	RD	Watanabe et al. (2015)

Table 1 *continued*

Table 1 (continued)

Source name	Source type	$T_{\text{ex}}(\text{N-COM})$	a (K)	$T_{\text{ex}}(\text{O-COM})$	b (K)	$T_{\text{ex}}(\text{CH}_3\text{CN})$	c (K)	$T_{\text{ex}}(\text{CH}_3\text{OH})$	d (K)	Sign of CGS e	Telescope	Analysis method f	Reference
NGC 6334-29	High mass	169 ± 4		285 ± 28	...	33 ± 1		127 ± 1	...	CSO	M	Widicus Weaver et al. (2017)	
NGC 6334-38	High mass	36 ± 2		45 ± 6	17 ± 2	16 ± 0		21 ± 0	...	CSO	M	Widicus Weaver et al. (2017)	
NGC 6334-43	High mass	33 ± 8		35 ± 3	...	20 ± 0		16 ± 0	yes	CSO	M	Widicus Weaver et al. (2017)	
NGC 6334-I(N)	High mass	22 ± 1		241 ± 35	n/a	178 ± 10		JCMT + IRAM 30m	RD	Bisschop et al. (2017)	
NGC 6334 IRS1	High mass	92 ₀ ³		116 ± 37	n/a	Nobeyama	RD	Suzuki et al. (2018)	
...	...	58 ± 23		313 ± 347	n/a	201 ± 24		Nobeyama	RD	Suzuki et al. (2018)	
NGC 6334 IRS1 F	High mass	83 ± 31		120 ± 32	n/a	ALMA	RD	Suzuki et al. (2019)	
NGC 6334 MM1	High mass	120 ± 11		157 ± 36	n/a	ALMA	RD	Suzuki et al. (2019)	
NGC 6334 MM2	High mass	137 ± 46		265 ₆₇ ¹³⁹	...	157 ₁₃ ¹⁵		yes	...	PdBI	RD	Fuente et al. (2014)	
NGC 7129 FIRS 2	Int. mass	405 ₆₇ ¹⁹⁰		265	...	238		yes	...	PdBI	M	Fuente et al. (2014)	
...	...	405		66 ± 14	n/a	n/a		yes	...	CSO	M	Widicus Weaver et al. (2017)	
NGC 7538-14-37	High mass	68 ± 56		60 ± 6	RD	Öberg et al. (2013)	
NGC 7538 IRS9	High mass	281 ± 218		60 ± 15	34 ± 2	RD	Öberg et al. (2013)	
...		111 ± 20	81 ± 16	RD	Fayolle et al. (2015)	
Orion KL	High mass	200		140 ± 10	RD	Johansson et al. (1984)	
...	...	285		120	RD	Sutton et al. (1985)	
...	...	445 ± 36		188 ± 3		yes	RD	Schilke et al. (1997)	
...	...	273		158		yes	RD	Lee et al. (2001)	
...	...	227 ± 21		599 ± 295	RD	White et al. (2003)	
...	...	250		220		yes	RD	Comito et al. (2005)	
...	...	655 ± 235		308 ± 42	229 ± 4	194 ± 2		yes	RD	Widicus Weaver et al. (2017)	
...	...	146 ± 28		183 ± 10	n/a	RD	Suzuki et al. (2018)	
...	...	122 ± 50		225 ± 23	n/a	RD	Suzuki et al. (2018)	
Orion KL hot core	High mass	133 ± 20		160 ± 10	n/a	RD	Ohishi et al. (1986)	
...	...	130		168	n/a	n/a		yes	RD	Sutton et al. (1995)	
...	...	93 ± 7		152	n/a	RD	Ikeda et al. (2001)	
...	...	239		360	n/a	303		RD	Schilke et al. (2001)	
...	...	137		178	Odin	RD	Person et al. (2007)	
...	...	300		128	260	...		yes	...	Herschel HIFI	M	Crockett et al. (2014)	
...	...	155 ± 16		225 ± 19	IRAM 30m + SMA	RD	Feng et al. (2015)	
Orion KL compact ridge	High mass	101 ± 9		146 ± 3	RD	Blake et al. (1987)	
...	...	125		105	n/a	n/a		yes	RD	Sutton et al. (1995)	
...	...	230		140		yes	...	Herschel HIFI	M	Crockett et al. (2014)	
SerpS-MM18a	Low mass	244 ± 28		238 ± 202	...	154 ± 22		yes	...	NOEMA	RD	Belloche et al. (2020)	
SerpS-MM18b	Low mass	17 ± 18		69 ± 10	NOEMA	RD	Belloche et al. (2020)	
Sgr B2(N)	High mass	440 ₉₀ ¹⁹⁰		197 ₂₂ ³¹	400 ₈₆ ¹⁰⁴	n/a		yes	...	SEST	RD	Nummelin et al. (2000)	
...	...	180 ± 89		148 ± 26	n/a	...		yes	...	NRO	RD	Ikeda et al. (2001)	
...	...	200		130	...	n/a		yes	...	IRAM 30m	M	Belloche et al. (2009)	
...	...	200		200	IRAM 30m	M	Belloche et al. (2013)	

Table 1 continued

Table 1 (continued)

Source name	Source type	$T_{\text{ex}}(\text{N-COM})^a$ (K)	$T_{\text{ex}}(\text{O-COM})^b$ (K)	$T_{\text{ex}}(\text{CH}_3\text{CN})^c$ (K)	$T_{\text{ex}}(\text{CH}_3\text{OH})^d$ (K)	Sign of CGS ^e	Telescope	Analysis method ^f	Reference
Sgr B2(N) N2	High mass	300	180	...	170	yes	Herschel HIFI	M	Neill et al. (2014)
...	High mass	253 ± 15	142 ± 4	...	n/a	yes	ALMA	RD	Belloche et al. (2016)
...	...	200	160	170	...	yes	ALMA	M	Belloche et al. (2016)
Sgr B2(N) N3	High mass	170	170	145	ALMA	M	Bonfand et al. (2017)
Sgr B2(N) N4	High mass	150	190	145	ALMA	M	Bonfand et al. (2017)
Sgr B2(N) N5	High mass	170	180	145	ALMA	M	Bonfand et al. (2017)
Sgr B2(M)	High mass	300	200	yes	IRAM 30m	M	Belloche et al. (2013)
...	...	350 ₁₄₀ ⁵¹⁰	240 ₁₆₀ ⁰	n/a	150	yes	SEST	RD	Nummelin et al. (2000)
Sgr B2(NW)	High mass	26 ₈ ¹⁹	40 ₈ ¹³	n/a	16 ₂ ⁴	...	SEST	RD	Nummelin et al. (2000)
SVS 4-5	Low mass	17 ± 2	20 ± 0	IRAM 30m	RD	Öberg et al. (2014); Bergner et al. (2017)
SVS13-A	Low mass	317 ± 136	285 ± 82	222 ± 49	...	yes	NOEMA	RD	Belloche et al. (2020)
W3(H2O)	High mass	375 ± 210	203 ± 8	yes	JCMT	RD	Heimlich & van Dishoeck (1997)
...	...	94 ₀ ¹⁶	189 ± 108	n/a	139 ± 8	...	JCMT + IRAM 30m	RD	Bisschop et al. (2007)
...	...	200	360	SMA	M	Qin et al. (2015)
...	178 ± 23	239 ± 12	152 ± 3	151 ± 1	CSO	M	Widicus Weaver et al. (2017)
W3(OH)	High mass	95	155	SMA	M	Qin et al. (2015)
W3 IRS5	High mass	92 ± 23	166 ± 85	IRAM 30m + SMA	RD	Fayolle et al. (2015)
W43-MM1 core 3	High mass	170 ± 70	320 ± 80	130 ± 60	ALMA	RD	Molet et al. (2019)
W51	High mass	226 ± 12	472 ± 23	...	257 ± 4	...	CSO	M	Widicus Weaver et al. (2017)
...	...	118 ± 38	197 ± 28	n/a	Nozeyama	RD	Suzuki et al. (2018)
...	...	106 ± 82	293 ± 62	n/a	Nozeyama	RD	Suzuki et al. (2018)
W51 e1/e2	High mass	236 ± 99	208	n/a	...	yes	NRO, NRAO	RD	Ikeda et al. (2001)
...	...	237 ± 48	174 ± 44	212 ± 8	143 ± 10	yes	OSO	RD	Kalenskii & Johansson (2010b)
W51 e2	High mass	114 ± 11	154 ± 8	n/a	IRAM 30m	RD	Demyk et al. (2008)
...	...	155 ± 98	94 ± 19	n/a	...	yes	ALMA	RD	Suzuki et al. (2019)
W51 e8	High mass	131 ± 51	205 ± 40	n/a	ALMA	RD	Suzuki et al. (2019)
W75N	High mass	169 ± 7	206 ± 2	CSO	M	Widicus Weaver et al. (2017)
144 ^g						64 ^h			

^aHighest excitation temperature among all N-bearing COMs in the study.^bHighest excitation temperature among all O-bearing COMs in the study.^cExcitation temperature of CH₃CN (or isotopologue) if this was not the highest temperature for all N-COMs, n/a means no T_{ex} is available for CH₃CN.^dExcitation temperature of CH₃OH (or isotopologue) if this was not the highest temperature for all O-COMs, n/a means no T_{ex} is available for CH₃OH.^eSign of carbon-grain sublimation, i.e., T_{ex} higher for N-COMs than O-COMs.^fMethod used to derive the excitation temperatures. Here we only make a broad distinction between rotational diagram analysis (RD) or spectral modeling (M).^gTotal number of entries.^hTotal number of entries showing a sign of carbon grain sublimation.

REFERENCES

- Agúndez, M., Marcelino, N., Cernicharo, J., Roueff, E., & Tafalla, M. 2019, A&A, 625, A147, doi: [10.1051/0004-6361/201935164](https://doi.org/10.1051/0004-6361/201935164)
- Allen, V., van der Tak, F. F. S., Sánchez-Monge, Á., Cesaroni, R., & Beltrán, M. T. 2017, A&A, 603, A133, doi: [10.1051/0004-6361/201629118](https://doi.org/10.1051/0004-6361/201629118)
- Allen, V., van der Tak, F. F. S., & Walsh, C. 2018, A&A, 616, A67, doi: [10.1051/0004-6361/201732553](https://doi.org/10.1051/0004-6361/201732553)
- Altweig, K., Balsiger, H., Hänni, N., et al. 2020, Nature Astronomy, 3, doi: [10.1038/s41550-019-0991-9](https://doi.org/10.1038/s41550-019-0991-9)
- Anderson, D. E., Bergin, E. A., Blake, G. A., et al. 2017, ApJ, 845, 13, doi: [10.3847/1538-4357/aa7da1](https://doi.org/10.3847/1538-4357/aa7da1)
- Aslam Siddiqui, M., Siddiqui, R. A., & Atakan, B. 2009, Journal of Chemical & Engineering Data, 54, 2795, doi: [10.1021/je9001653](https://doi.org/10.1021/je9001653)
- Beaklini, P. P. B., Mendoza, E., Canelo, C. M., et al. 2020, MNRAS, 491, 427, doi: [10.1093/mnras/stz3024](https://doi.org/10.1093/mnras/stz3024)
- Belloche, A., Garrod, R. T., Müller, H. S. P., et al. 2009, A&A, 499, 215, doi: [10.1051/0004-6361/200811550](https://doi.org/10.1051/0004-6361/200811550)
- Belloche, A., Müller, H. S. P., Garrod, R. T., & Menten, K. M. 2016, A&A, 587, A91, doi: [10.1051/0004-6361/201527268](https://doi.org/10.1051/0004-6361/201527268)
- Belloche, A., Müller, H. S. P., Menten, K. M., Schilke, P., & Comito, C. 2013, A&A, 559, A47, doi: [10.1051/0004-6361/201321096](https://doi.org/10.1051/0004-6361/201321096)
- Belloche, A., Maury, A. J., Maret, S., et al. 2020, arXiv e-prints, arXiv:2002.00592. <https://arxiv.org/abs/2002.00592>
- Bergin, E. A., Blake, G. A., Ciesla, F., Hirschmann, M. M., & Li, J. 2015, Proceedings of the National Academy of Science, 112, 8965, doi: [10.1073/pnas.1500954112](https://doi.org/10.1073/pnas.1500954112)
- Bergin, E. A., & Cleeves, L. I. 2018, Chemistry During the Gas-Rich Stage of Planet Formation, 137, doi: [10.1007/978-3-319-55333-7_137](https://doi.org/10.1007/978-3-319-55333-7_137)
- Bergin, E. A., & Snell, R. L. 2002, ApJL, 581, L105, doi: [10.1086/346014](https://doi.org/10.1086/346014)
- Bergner, J. B., Öberg, K. I., Garrod, R. T., & Graninger, D. M. 2017, ApJ, 841, 120, doi: [10.3847/1538-4357/aa72f6](https://doi.org/10.3847/1538-4357/aa72f6)
- Bergner, J. B., Öberg, K. I., Rajappan, M., & Fayolle, E. C. 2016, ApJ, 829, 85, doi: [10.3847/0004-637X/829/2/85](https://doi.org/10.3847/0004-637X/829/2/85)
- Bisschop, S. E., Jørgensen, J. K., van Dishoeck, E. F., & de Wachter, E. B. M. 2007, A&A, 465, 913, doi: [10.1051/0004-6361:20065963](https://doi.org/10.1051/0004-6361:20065963)
- Blake, G. A., Sutton, E. C., Masson, C. R., & Phillips, T. G. 1987, ApJ, 315, 621, doi: [10.1086/165165](https://doi.org/10.1086/165165)
- Bøgelund, E. G., Barr, A. G., Taquet, V., et al. 2019, A&A, 628, A2, doi: [10.1051/0004-6361/201834527](https://doi.org/10.1051/0004-6361/201834527)
- Bonfand, M., Belloche, A., Menten, K. M., Garrod, R. T., & Müller, H. S. P. 2017, A&A, 604, A60, doi: [10.1051/0004-6361/201730648](https://doi.org/10.1051/0004-6361/201730648)
- Bossa, J. B., Theulé, P., Duvernay, F., Borget, F., & Chiavassa, T. 2008, A&A, 492, 719, doi: [10.1051/0004-6361:200810536](https://doi.org/10.1051/0004-6361:200810536)
- Brouillet, N., Despois, D., Lu, X. H., et al. 2015, A&A, 576, A129, doi: [10.1051/0004-6361/201424588](https://doi.org/10.1051/0004-6361/201424588)
- Calcutt, H., Jørgensen, J. K., Müller, H. S. P., et al. 2018a, A&A, 616, A90, doi: [10.1051/0004-6361/201732289](https://doi.org/10.1051/0004-6361/201732289)
- Calcutt, H., Fiechter, M. R., Willis, E. R., et al. 2018b, A&A, 617, A95, doi: [10.1051/0004-6361/201833140](https://doi.org/10.1051/0004-6361/201833140)
- Caselli, P., Hasegawa, T. I., & Herbst, E. 1993, ApJ, 408, 548, doi: [10.1086/172612](https://doi.org/10.1086/172612)
- Caselli, P., Keto, E., Bergin, E. A., et al. 2012, ApJL, 759, L37, doi: [10.1088/2041-8205/759/2/L37](https://doi.org/10.1088/2041-8205/759/2/L37)
- Cazaux, S., Tielens, A. G. G. M., Ceccarelli, C., et al. 2003, ApJL, 593, L51, doi: [10.1086/378038](https://doi.org/10.1086/378038)
- Charnley, S. B., Tielens, A. G. G. M., & Millar, T. J. 1992, ApJL, 399, L71, doi: [10.1086/186609](https://doi.org/10.1086/186609)
- Churchwell, E., Wood, D., Myers, P. C., & Myers, R. V. 1986, ApJ, 305, 405, doi: [10.1086/164256](https://doi.org/10.1086/164256)
- Cieza, L. A., Casassus, S., Tobin, J., et al. 2016, Nature, 535, 258, doi: [10.1038/nature18612](https://doi.org/10.1038/nature18612)
- Clementi, E., & Gayles, J. N. 1967, JChPh, 47, 3837, doi: [10.1063/1.1701543](https://doi.org/10.1063/1.1701543)
- Comito, C., Schilke, P., Phillips, T. G., et al. 2005, ApJS, 156, 127, doi: [10.1086/425996](https://doi.org/10.1086/425996)
- Coutens, A., Willis, E. R., Garrod, R. T., et al. 2018, A&A, 612, A107, doi: [10.1051/0004-6361/201732346](https://doi.org/10.1051/0004-6361/201732346)
- Crockett, N. R., Bergin, E. A., Neill, J. L., et al. 2015, ApJ, 806, 239, doi: [10.1088/0004-637X/806/2/239](https://doi.org/10.1088/0004-637X/806/2/239)
- . 2014, ApJ, 787, 112, doi: [10.1088/0004-637X/787/2/112](https://doi.org/10.1088/0004-637X/787/2/112)
- Csengeri, T., Belloche, A., Bontemps, S., et al. 2019, A&A, 632, A57, doi: [10.1051/0004-6361/201935226](https://doi.org/10.1051/0004-6361/201935226)
- D'Alessio, P., Calvet, N., & Woolum, D. S. 2005, in Astronomical Society of the Pacific Conference Series, Vol. 341, Chondrites and the Protoplanetary Disk, ed. A. N. Krot, E. R. D. Scott, & B. Reipurth, 353
- Danger, G., Borget, F., Chomat, M., et al. 2011, A&A, 535, A47, doi: [10.1051/0004-6361/201117602](https://doi.org/10.1051/0004-6361/201117602)
- Demyk, K., Włodarczak, G., & Carvajal, M. 2008, A&A, 489, 589, doi: [10.1051/0004-6361:200809354](https://doi.org/10.1051/0004-6361:200809354)
- Evans, Neal J., I., Dunham, M. M., Jørgensen, J. K., et al. 2009, ApJS, 181, 321, doi: [10.1088/0067-0049/181/2/321](https://doi.org/10.1088/0067-0049/181/2/321)
- Favre, C., Pagani, L., Goldsmith, P. F., et al. 2017, A&A, 604, L2, doi: [10.1051/0004-6361/201731327](https://doi.org/10.1051/0004-6361/201731327)

- Fayolle, E. C., Öberg, K. I., Garrod, R. T., van Dishoeck, E. F., & Bisschop, S. E. 2015, A&A, 576, A45, doi: [10.1051/0004-6361/201323114](https://doi.org/10.1051/0004-6361/201323114)
- Feng, S., Beuther, H., Henning, T., et al. 2015, A&A, 581, A71, doi: [10.1051/0004-6361/201322725](https://doi.org/10.1051/0004-6361/201322725)
- Finocchi, F., Gail, H. P., & Duschl, W. J. 1997, A&A, 325, 1264
- Fischer, R. A., Cottrell, E., Hauri, E., Lee, K. K. M., & Le Voyer, M. 2020, Proceedings of the National Academy of Sciences, 117, 8743, doi: [10.1073/pnas.1919930117](https://doi.org/10.1073/pnas.1919930117)
- Fontani, F., Pascucci, I., Caselli, P., et al. 2007, A&A, 470, 639, doi: [10.1051/0004-6361:20077485](https://doi.org/10.1051/0004-6361:20077485)
- Friedel, D. N., & Snyder, L. E. 2008, ApJ, 672, 962, doi: [10.1086/523896](https://doi.org/10.1086/523896)
- Fu, L., & Lin, G.-M. 2016, Research in Astronomy and Astrophysics, 16, 182, doi: [10.1088/1674-4527/16/12/182](https://doi.org/10.1088/1674-4527/16/12/182)
- Fuente, A., Cernicharo, J., Caselli, P., et al. 2014, A&A, 568, A65, doi: [10.1051/0004-6361/201323074](https://doi.org/10.1051/0004-6361/201323074)
- Gail, H.-P., & Trieloff, M. 2017, A&A, 606, A16, doi: [10.1051/0004-6361/201730480](https://doi.org/10.1051/0004-6361/201730480)
- Garrod, R. T. 2013, ApJ, 765, 60, doi: [10.1088/0004-637X/765/1/60](https://doi.org/10.1088/0004-637X/765/1/60)
- Garrod, R. T., Widicus Weaver, S. L., & Herbst, E. 2008, ApJ, 682, 283, doi: [10.1086/588035](https://doi.org/10.1086/588035)
- Geers, V. C., van Dishoeck, E. F., Pontoppidan, K. M., et al. 2009, A&A, 495, 837, doi: [10.1051/0004-6361:200811001](https://doi.org/10.1051/0004-6361:200811001)
- Geiss, J. 1987, A&A, 187, 859
- Gibb, E., Nummelin, A., Irvine, W. M., Whittet, D. C. B., & Bergman, P. 2000, ApJ, 545, 309, doi: [10.1086/317805](https://doi.org/10.1086/317805)
- Gieser, C., Semenov, D., Beuther, H., et al. 2019, A&A, 631, A142, doi: [10.1051/0004-6361/201935865](https://doi.org/10.1051/0004-6361/201935865)
- Goldfarb, J. L., & Suuberg, E. M. 2008, Journal of Chemical & Engineering Data, 53, 670, doi: [10.1021/je7005133](https://doi.org/10.1021/je7005133)
- Hartmann, L., & Kenyon, S. J. 1996, ARA&A, 34, 207, doi: [10.1146/annurev.astro.34.1.207](https://doi.org/10.1146/annurev.astro.34.1.207)
- Hatchell, J., Thompson, M. A., Millar, T. J., & MacDonald, G. H. 1998, A&AS, 133, 29, doi: [10.1051/aas:1998309](https://doi.org/10.1051/aas:1998309)
- Helmich, F. P., & van Dishoeck, E. F. 1997, A&AS, 124, 205, doi: [10.1051/aas:1997357](https://doi.org/10.1051/aas:1997357)
- Hsieh, T.-H., Murillo, N. M., Belloche, A., et al. 2019, ApJ, 884, 149, doi: [10.3847/1538-4357/ab425a](https://doi.org/10.3847/1538-4357/ab425a)
- Ikeda, M., Ohishi, M., Nummelin, A., et al. 2001, ApJ, 560, 792, doi: [10.1086/322957](https://doi.org/10.1086/322957)
- Isokoski, K., Bottinelli, S., & van Dishoeck, E. F. 2013, A&A, 554, A100, doi: [10.1051/0004-6361/201220959](https://doi.org/10.1051/0004-6361/201220959)
- Jensen, A. G., Rachford, B. L., & Snow, T. P. 2007, ApJ, 654, 955, doi: [10.1086/509096](https://doi.org/10.1086/509096)
- Jessberger, E. K., Christoforidis, A., & Kissel, J. 1988, Nature, 332, 691, doi: [10.1038/332691a0](https://doi.org/10.1038/332691a0)
- Jiménez-Serra, I., Zhang, Q., Viti, S., Martín-Pintado, J., & de Wit, W. J. 2012, ApJ, 753, 34, doi: [10.1088/0004-637X/753/1/34](https://doi.org/10.1088/0004-637X/753/1/34)
- Johansson, L. E. B., Andersson, C., Ellder, J., et al. 1984, A&A, 130, 227
- Johnstone, D., Hendricks, B., Herczeg, G. J., & Bruderer, S. 2013, ApJ, 765, 133, doi: [10.1088/0004-637X/765/2/133](https://doi.org/10.1088/0004-637X/765/2/133)
- Jørgensen, J. K., Visser, R., Williams, J. P., & Bergin, E. A. 2015, A&A, 579, A23, doi: [10.1051/0004-6361/201425317](https://doi.org/10.1051/0004-6361/201425317)
- Jørgensen, J. K., Müller, H. S. P., Calcutt, H., et al. 2018, A&A, 620, A170, doi: [10.1051/0004-6361/201731667](https://doi.org/10.1051/0004-6361/201731667)
- Jura, M. 2006, ApJ, 653, 613, doi: [10.1086/508738](https://doi.org/10.1086/508738)
- Kalenskii, S. V., & Johansson, L. E. B. 2010a, Astronomy Reports, 54, 295, doi: [10.1134/S1063772910040037](https://doi.org/10.1134/S1063772910040037)
- . 2010b, Astronomy Reports, 54, 1084, doi: [10.1134/S1063772910120036](https://doi.org/10.1134/S1063772910120036)
- Klarmann, L., Ormel, C. W., & Dominik, C. 2018, A&A, 618, L1, doi: [10.1051/0004-6361/201833719](https://doi.org/10.1051/0004-6361/201833719)
- Kress, M. E., Tielens, A. G. G. M., & Frenklach, M. 2010, Advances in Space Research, 46, 44, doi: [10.1016/j.asr.2010.02.004](https://doi.org/10.1016/j.asr.2010.02.004)
- Lee, C. W., Cho, S.-H., & Lee, S.-M. 2001, ApJ, 551, 333, doi: [10.1086/320062](https://doi.org/10.1086/320062)
- Lee, J.-E. 2007, Journal of Korean Astronomical Society, 40, 83, doi: [10.5303/JKAS.2007.40.4.083](https://doi.org/10.5303/JKAS.2007.40.4.083)
- Lee, J.-E., Bergin, E. A., & Nomura, H. 2010, ApJL, 710, L21, doi: [10.1088/2041-8205/710/1/L21](https://doi.org/10.1088/2041-8205/710/1/L21)
- Lee, J.-E., Lee, S., Baek, G., et al. 2019, Nature Astronomy, 3, 314, doi: [10.1038/s41550-018-0680-0](https://doi.org/10.1038/s41550-018-0680-0)
- Lodders, K. 2010, Astrophysics and Space Science Proceedings, 16, 379, doi: [10.1007/978-3-642-10352-0_8](https://doi.org/10.1007/978-3-642-10352-0_8)
- MacDonald, G. H., Gibb, A. G., Habing, R. J., & Millar, T. J. 1996, A&AS, 119, 333
- Manigand, S., Jørgensen, J. K., Calcutt, H., et al. 2020, A&A, 635, A48, doi: [10.1051/0004-6361/201936299](https://doi.org/10.1051/0004-6361/201936299)
- Manske, V., & Henning, T. 1999, A&A, 349, 907
- Marty, B. 2012, Earth and Planetary Science Letters, 313, 56, doi: [10.1016/j.epsl.2011.10.040](https://doi.org/10.1016/j.epsl.2011.10.040)
- McGuire, B. A., Burkhardt, A. M., Kalenskii, S., et al. 2018, Science, 359, 202, doi: [10.1126/science.aaq4890](https://doi.org/10.1126/science.aaq4890)
- Mendoza, E., Bronfman, L., Duronea, N. U., et al. 2018, ApJ, 853, 152, doi: [10.3847/1538-4357/aaa1ec](https://doi.org/10.3847/1538-4357/aaa1ec)
- Mishra, A., & Li, A. 2015, ApJ, 809, 120, doi: [10.1088/0004-637X/809/2/120](https://doi.org/10.1088/0004-637X/809/2/120)
- Molet, J., Brouillet, N., Nony, T., et al. 2019, A&A, 626, A132, doi: [10.1051/0004-6361/201935497](https://doi.org/10.1051/0004-6361/201935497)
- Mookerjea, B., Casper, E., Mundy, L. G., & Looney, L. W. 2007, ApJ, 659, 447, doi: [10.1086/512095](https://doi.org/10.1086/512095)

- Nakano, H., Kouchi, A., Tachibana, S., & Tsuchiyama, A. 2003, ApJ, 592, 1252, doi: [10.1086/375856](https://doi.org/10.1086/375856)
- Neill, J. L., Bergin, E. A., Lis, D. C., et al. 2014, ApJ, 789, 8, doi: [10.1088/0004-637X/789/1/8](https://doi.org/10.1088/0004-637X/789/1/8)
- Nieva, M. F., & Przybilla, N. 2012, A&A, 539, A143, doi: [10.1051/0004-6361/201118158](https://doi.org/10.1051/0004-6361/201118158)
- Noble, J. A., Theule, P., Borget, F., et al. 2013, MNRAS, 428, 3262, doi: [10.1093/mnras/sts272](https://doi.org/10.1093/mnras/sts272)
- Nummelin, A., Bergman, P., Hjalmarson, Å., et al. 2000, ApJS, 128, 213, doi: [10.1086/313376](https://doi.org/10.1086/313376)
- Öberg, K. I., Boamah, M. D., Fayolle, E. C., et al. 2013, ApJ, 771, 95, doi: [10.1088/0004-637X/771/2/95](https://doi.org/10.1088/0004-637X/771/2/95)
- Öberg, K. I., Lauck, T., & Graninger, D. 2014, ApJ, 788, 68, doi: [10.1088/0004-637X/788/1/68](https://doi.org/10.1088/0004-637X/788/1/68)
- Ohishi, M., Kaifu, N., Suzuki, H., & Morimoto, M. 1986, Ap&SS, 118, 405, doi: [10.1007/BF00651157](https://doi.org/10.1007/BF00651157)
- Ospina-Zamudio, J., Lefloch, B., Ceccarelli, C., et al. 2018, A&A, 618, A145, doi: [10.1051/0004-6361/201832857](https://doi.org/10.1051/0004-6361/201832857)
- Palau, A., Walsh, C., Sánchez-Monge, Á., et al. 2017, MNRAS, 467, 2723, doi: [10.1093/mnras/stx004](https://doi.org/10.1093/mnras/stx004)
- Peng, T. C., Despois, D., Brouillet, N., et al. 2013, A&A, 554, A78, doi: [10.1051/0004-6361/201220891](https://doi.org/10.1051/0004-6361/201220891)
- Persson, C. M., Olofsson, A. O. H., Koning, N., et al. 2007, A&A, 476, 807, doi: [10.1051/0004-6361:20077225](https://doi.org/10.1051/0004-6361:20077225)
- Poch, O., Istiqomah, I., Quirico, E., et al. 2020, Science, 367, aaw7462, doi: [10.1126/science.aaw7462](https://doi.org/10.1126/science.aaw7462)
- Poteet, C. A., Whittet, D. C. B., & Draine, B. T. 2015, ApJ, 801, 110, doi: [10.1088/0004-637X/801/2/110](https://doi.org/10.1088/0004-637X/801/2/110)
- Qin, S.-L., Schilke, P., Wu, J., et al. 2015, ApJ, 803, 39, doi: [10.1088/0004-637X/803/1/39](https://doi.org/10.1088/0004-637X/803/1/39)
- Qin, S.-L., Wu, Y., Huang, M., et al. 2010, ApJ, 711, 399, doi: [10.1088/0004-637X/711/1/399](https://doi.org/10.1088/0004-637X/711/1/399)
- Raunier, S., Chiavassa, T., Marinelli, F., & Aycard, J.-P. 2004, Chemical Physics, 302, 259, doi: [10.1016/j.chemphys.2004.04.013](https://doi.org/10.1016/j.chemphys.2004.04.013)
- Remusat, L. 2014, BIO Web of Conferences, 2, 03001, doi: [10.1051/bioconf/20140203001](https://doi.org/10.1051/bioconf/20140203001)
- Rice, T. S., Bergin, E. A., Jørgensen, J. K., & Wampfler, S. F. 2018, ApJ, 866, 156, doi: [10.3847/1538-4357/aadfdb](https://doi.org/10.3847/1538-4357/aadfdb)
- Rodgers, S. D., & Charnley, S. B. 2001, ApJ, 546, 324, doi: [10.1086/318263](https://doi.org/10.1086/318263)
- Rubin, M., Altweig, K., Balsiger, H., et al. 2019, MNRAS, 489, 594, doi: [10.1093/mnras/stz2086](https://doi.org/10.1093/mnras/stz2086)
- Schilke, P., Benford, D. J., Hunter, T. R., Lis, D. C., & Phillips, T. G. 2001, ApJS, 132, 281, doi: [10.1086/318951](https://doi.org/10.1086/318951)
- Schilke, P., Groesbeck, T. D., Blake, G. A., Phillips, & T. G. 1997, ApJS, 108, 301, doi: [10.1086/312948](https://doi.org/10.1086/312948)
- Scholz, A., Froebrich, D., & Wood, K. 2013, MNRAS, 430, 2910, doi: [10.1093/mnras/stt091](https://doi.org/10.1093/mnras/stt091)
- Sutton, E. C., Blake, G. A., Masson, C. R., & Phillips, T. G. 1985, ApJS, 58, 341, doi: [10.1086/191045](https://doi.org/10.1086/191045)
- Sutton, E. C., Peng, R., Danchi, W. C., et al. 1995, ApJS, 97, 455, doi: [10.1086/192147](https://doi.org/10.1086/192147)
- Suzuki, T., Ohishi, M., Saito, M., et al. 2018, ApJS, 237, 3, doi: [10.3847/1538-4365/aac8db](https://doi.org/10.3847/1538-4365/aac8db)
- Suzuki, T., Majumdar, L., Tokuda, K., et al. 2019, arXiv e-prints, arXiv:1909.00528
<https://arxiv.org/abs/1909.00528>
- Taniguchi, K., Saito, M., Majumdar, L., et al. 2018, ApJ, 866, 150, doi: [10.3847/1538-4357/aade97](https://doi.org/10.3847/1538-4357/aade97)
- Taquet, V., López-Sepulcre, A., Ceccarelli, C., et al. 2015, ApJ, 804, 81, doi: [10.1088/0004-637X/804/2/81](https://doi.org/10.1088/0004-637X/804/2/81)
- Tielens, A. G. G. M. 2011, in IAU Symposium, Vol. 280, The Molecular Universe, ed. J. Cernicharo & R. Bachiller, 3–18, doi: [10.1017/S1743921311024823](https://doi.org/10.1017/S1743921311024823)
- van Dishoeck, E. F., & van der Tak, F. F. S. 2000, in IAU Symposium, Vol. 197, From Molecular Clouds to Planetary, ed. Y. C. Minh & E. F. van Dishoeck, 97, <https://arxiv.org/abs/astro-ph/0002098>
- Vinogradoff, V., Duvernay, F., Danger, G., Theulé, P., & Chiavassa, T. 2011, A&A, 530, A128, doi: [10.1051/0004-6361/201116688](https://doi.org/10.1051/0004-6361/201116688)
- Visser, R., & Bergin, E. A. 2012, ApJL, 754, L18, doi: [10.1088/2041-8205/754/1/L18](https://doi.org/10.1088/2041-8205/754/1/L18)
- Visser, R., Bergin, E. A., & Jørgensen, J. K. 2015, A&A, 577, A102, doi: [10.1051/0004-6361/201425365](https://doi.org/10.1051/0004-6361/201425365)
- Wasson, J. T., & Kallemeyn, G. W. 1988, Philosophical Transactions of the Royal Society of London Series A, 325, 535, doi: [10.1098/rsta.1988.0066](https://doi.org/10.1098/rsta.1988.0066)
- Watanabe, Y., Sakai, N., López-Sepulcre, A., et al. 2015, ApJ, 809, 162, doi: [10.1088/0004-637X/809/2/162](https://doi.org/10.1088/0004-637X/809/2/162)
- Wei, C.-E., Nomura, H., Lee, J.-E., et al. 2019, ApJ, 870, 129, doi: [10.3847/1538-4357/aaf390](https://doi.org/10.3847/1538-4357/aaf390)
- White, G. J., Araki, M., Greaves, J. S., Ohishi, M., & Higginbottom, N. S. 2003, A&A, 407, 589, doi: [10.1051/0004-6361:20030841](https://doi.org/10.1051/0004-6361:20030841)
- Whittet, D. C. B. 2010, ApJ, 710, 1009, doi: [10.1088/0004-637X/710/2/1009](https://doi.org/10.1088/0004-637X/710/2/1009)
- Whidicus Weaver, S. L., Laas, J. C., Zou, L., et al. 2017, ApJS, 232, 3, doi: [10.3847/1538-4365/aa8098](https://doi.org/10.3847/1538-4365/aa8098)
- Wong, W.-H., & An, T. 2018, Research in Astronomy and Astrophysics, 18, 134, doi: [10.1088/1674-4527/18/11/134](https://doi.org/10.1088/1674-4527/18/11/134)
- Wyrowski, F., Schilke, P., Walmsley, C. M., & Menten, K. M. 1999, ApJL, 514, L43, doi: [10.1086/311934](https://doi.org/10.1086/311934)
- Yoshida, K., Sakai, N., Nishimura, Y., et al. 2019, PASJ, 71, S18, doi: [10.1093/pasj/pssy136](https://doi.org/10.1093/pasj/pssy136)